Recognizing Pain in Motor Imagery EEG Recordings Using Dynamic Functional Connectivity Graphs

Foroogh Shamsi, Ali Haddad, and Laleh Najafizadeh

Abstract— **The goal of this paper is to investigate whether motor imagery tasks, performed under pain-free versus pain conditions, can be discriminated from electroencephalography (EEG) recordings. Four motor imagery classes of right hand, left hand, foot, and tongue are considered. A functional connectivity-based feature extraction approach along with a long short-term memory (LSTM) classifier are employed for classifying pain-free versus under-pain classes. Moreover, classification is performed in different frequency bands to study the significance of each band in differentiating motor imagery data associated with pain-free and under-pain states. When considering all frequency bands, the average classification accuracy is in the range of $77.86-80.04\%$. Our frequency-specific analysis shows that the gamma band results in a notably higher accuracy than other bands, indicating the importance of this band in discriminating pain/no-pain conditions during the execution of motor imagery tasks. In contrast, functional connectivity graphs extracted from delta and theta bands do not seem to provide discriminatory information between pain-free and under-pain conditions. This is the first study demonstrating that motor imagery tasks executed under pain and without pain conditions can be discriminated from EEG recordings. Our findings can provide new insights for developing effective brain computer interface-based assistive technologies for patients who are in real need of them.**

I. INTRODUCTION

Brain computer interface (BCI)-based assistive technologies can help patients suffering from communication and motor function disorders to express their feelings, and to perform simple activities of their daily life independently. The goal of a BCI in such technologies is to generate control signals directly from mentally-modulated brain activity, in order to enable the operation of assistive devices [1]. Electroencephalography (EEG) is a great candidate for monitoring brain activity in BCI applications, due to its low-cost, portability, and non-invasiveness properties [2], [3]. A large number of EEG-based BCI studies have considered some forms of motor imagery tasks as their paradigm, and promising results have been reported for this paradigm in individuals with motor disabilities such as those with spinal cord injury, and amyotrophic lateral sclerosis (ALS) [4], [5].

Pain is, unfortunately, a major problem in a large group of patients who are in real need for BCI-based assistive technologies. For example, it has been reported that an estimated 80% of patients with spinal cord injury experience pain [6]. During the first year after the injury, in about $40-50\%$ of the patients the pain tends to become chronic [7].

Pain has been demonstrated to activate several regions in the brain including the prefrontal and somatosensory cortices. In [8], it has been reported that an increase in pain perception is associated with an increase in the gamma and theta powers in the medial prefrontal cortex as well as a decrease in the lower beta power in the contralateral sensorimotor cortex. In [9], a global reduction in power was observed in the lower spectral range. In [10], the relationship between the peak frequency of alpha activity over sensorimotor cortex and pain intensity was investigated, where it was shown that slower peak frequency in pain-free state is associated with higher predisposition of pain during pain condition. Results of these studies along with the prevalence of the pain in patients in need of the BCI technology, show the importance of incorporating this issue in the development of BCIs. In other words, BCIs designed for these patients should be adapted to take the pain conditions into account. This issue motivates for investigating whether the pain can be recognized in BCIs.

Previous studies on pain classification using EEG data focused on discriminating painful and non-painful stimulus in resting state [9]–[11], or aimed to classify various levels of low and high pain intensities [8], [12]. In this work, we focus on investigating pain in a task-based framework. We aim to examine if motor imagery tasks, performed in the presence of the pain, can be discriminated from pain-free motor imagery tasks. To achieve this goal, an experiment for collecting EEG recordings under both pain-free and pain conditions is designed. Four types of motor imagery tasks, commonly-used in BCIs, are considered. A dynamic functional connectivity graph-based approach [13] is taken to extract features for the classification problem. These dynamic features are fed to a long short term memory (LSTM) network in order to use the information in the graphs as well as their dynamics.

Moreover, evidence suggests that the experience of pain can affect the spectral properties of brain activity [14]. This motivates us to also perform frequency-specific analysis for the classification of motor imagery data under pain-free versus pain conditions. EEG data is decomposed into different bands of delta ($[1-4]$ Hz), theta ($[4-8]$ Hz), alpha ($[8-16]$ Hz), beta ($[16-32]$ Hz), and gamma ($[32-50]$ Hz) using discrete stationary wavelet transform (SWT), and signals from each of these bands are passed to the feature extraction and classification algorithms. The results of this study yield to better understanding of whether the presence

This work was supported by NSF award 1841087.

Authors are with Integrated Systems and Neuroimaging Laboratory, Department of Electrical and Computer Engineering, Rutgers University, Piscataway, NJ 08854, USA. {foroogh.shamsi, ali.haddad, laleh.najafizadeh}@rutgers.edu.

of pain impacts motor imagery-related EEG signals.

The rest of the paper is organized as follows. The experimental paradigm and data analysis are described in Section II. Results and discussions are presented in Sections III and IV, respectively and Section V concludes the paper.

II. MATERIALS AND METHODS

A. Data Collection

Four healthy and right-handed volunteers were recruited for this study. EEG data was recorded using a 32-channel EEG system (Brain Products, positioned based on the international $10-5$ electrode placement system), at a rate of 500 samples/s. Written informed consents approved by the Rutgers' Institutional Review Board (IRB) were obtained prior to the experiments.

Painful stimuli were delivered to the subjects' dorsum of the left hand using a standard 30×30 mm thermode (TSA-II, Medoc System) (see Fig. 1a). As there exists pain threshold and tolerance variability across subjects, for each subject, temperatures associated with the threshold and tolerance were determined prior to the main experiment.

To measure the pain threshold, while the thermode was in place, the temperature was increased from the baseline (32°C) with the rate of 1°C/s. Subjects were instructed to press a button on a response unit to indicate the moment that the temperature becomes painful to them. The temperature was then decreased to the baseline at the rate of 1°C/s. For determining the tolerance temperature, the rate of increasing the temperature was set to 1.5°C/s. Subjects were asked to press the button when pain becomes intolerable after which the thermode was cooled down to the baseline temperature at the rate of 8°C/s. The safety temperature limit of 50°C was considered for both the threshold and tolerance measurements. A total of eight trials were recorded for each case. Temperatures associated with the threshold and tolerance were determined by averaging the results across their corresponding trials. The average of the threshold and tolerance temperatures was set as the temperature of the pain stimulus (T_p). During the main experiment, random temperature points in the range of $[T_p-1, T_p+1]$ were selected to induce pain in different blocks of the experiment.

Additionally, to ensure that the highest temperature that was selected to be used for inducing pain in the main experiment, was bearable for subjects, the temperature was held for up to 6.5 minutes, which is equal to the maximum duration of the blocks in the experiment (see Section II-B). Subjects were instructed to press a button anytime during the 6.5 minutes interval, if they could not tolerate the pain. The idea was to reduce the maximum duration of the blocks (and increase the number of the blocks) if subjects could not tolerate the pain for a specified duration of the experiment. For all subjects, the obtained stimulus temperature was in the range of $(44.8-46.4)$°C. All subjects were able to tolerate the induced pain for the duration of 6.5 minutes.

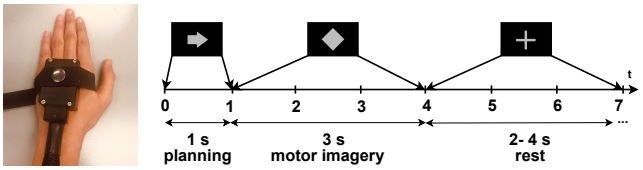

(a) (b)

Fig. 1: (a): To induce pain, thermode is attached to the subject's dorsum of the left hand. (b): Visual illustration of a single trial of the paradigm.

B. Experimental Paradigm

The main experiment consisted of 12 pain-free and under-pain blocks (6 blocks for each condition), which were presented in random order. During the under-pain blocks, the thermode was heated up to a random temperature in the range of the $[T_p-1, T_p+1]$. During the pain-free blocks, the temperature of the thermode was set to the baseline (32°C).

In order to avoid habituation to the heat, the location of the thermode was slightly moved on the dorsum of the left hand, for different blocks of the experiment. Moreover, to ensure that the subject does not feel temperature changes at the beginning/end of each block, we made sure the thermode had reached the targeted temperature (either baseline for the pain-free blocks or the stimulus temperatures for the under-pain blocks), before positioning it on the hand. The thermode was also detached from subject's hand at the end of each block before cooling it down.

Fig. 1b shows a visual illustration of the paradigm in each trial. At the beginning of the trial, an arrow is displayed for 1 s on the screen. The direction of the arrow is used to indicate the type of motor imagery task that subjects are expected to perform during the trial, i.e. right hand, left hand, foot, and tongue motor imagery tasks if the arrow points to right, left, down, or up directions, respectively. Next, a diamond symbol is displayed for 3 s. Subjects were instructed to start the imagery tasks as soon as they see the diamond symbol until it is disappeared from the screen. This is followed by a $2-4$ s inter-trial rest. Each block consisted of 12 trials for each motor imagery task. Therefore, at the end of the experiment, for each task, 72 trials for pain-free, and 72 trials for under-pain conditions are obtained. The duration of each block was about $4.8-6.4$ minutes.

C. Data Analysis

1) Preprocessing: From each trial, the first 4 s post-stimulus EEG data was extracted and preprocessed using the EEGLAB toolbox [15]. First, the data was filtered using a $[1,50]$ Hz band-pass finite impulse response (FIR) filter. Artifacts were then removed using independent component analysis (ICA).

2) Spectral Decomposition: For analyzing the data in different frequency bands, EEG recordings were decomposed into the bands of delta, theta, alpha, beta, and gamma using SWT. We considered SWT in this step, since it outperforms other regular filter-bank methods for capturing the

TABLE I: Accuracy results for classifying different motor imagery tasks under pain-free versus pain conditions.

	Right Hand	**Left Hand**	**Foot**	**Tongue**	**Average**
Subject 1	85.65 ± 8.10	82.13 ± 9.02	$\mathbf{88.16 \pm 8.40}$	78.54 ± 9.02	83.62 ± 8.64
Subject 2	78.57 ± 10.66	73.01 ± 9.39	76.56 ± 12.06	76.78 ± 9.79	76.23 ± 10.52
Subject 3	76.56 ± 9.18	76.01 ± 8.82	75.42 ± 8.88	72.42 ± 9.78	75.10 ± 9.18
Subject 4	76.94 ± 7.92	81.92 ± 7.51	80.01 ± 9.79	83.69 ± 9.19	80.64 ± 8.65
Average	79.43 ± 9.03	78.26 ± 8.72	80.04 ± 9.89	77.86 ± 9.46	$\mathbf{78.90 \pm 9.28}$

temporal structure of the signals. We used Daubechies 4 (Db4) wavelet, due to its similarity to the underlying EEG activity [16] and the orthogonality of the corresponding basis [17]. Signals reconstructed from each band are passed to the feature extraction algorithm to find their corresponding functional connectivity graphs, and to form the feature vectors associated with each band.

3) Feature Extraction: We employed our recently proposed feature extraction method [13] to extract features based on dynamic functional connectivity networks from EEG recordings. This method consists of two main steps. First, the EEG data is segmented into variable-length segments during which the spatial distribution of the underlying functional networks stays quasi-stationary. In this method, the segment boundaries are identified when the spatial patterns of functional connectivity networks are changed as assessed based on the results of KolmogorovSmirnov statistical test [18], [19]. It should be noted that since the nodes of the graphs are the EEG electrodes, the problem of volume conduction is addressed by applying the surface Laplacian operator [20]–[22] on the EEG data. Moreover, the segment-wise average value of each EEG channel is subtracted from the data points of the corresponding segment to detect functional networks based on the patterns of their temporal activities rather than detecting the nodes with the highest average intensities. In the second step, functional networks sustaining their connectivity during each extracted segment are identified and the corresponding undirected graphs are constructed. Then, these graphs are vectorized and used as features for the classification problem. For more details on the feature extraction method refer to [13].

4) Classification: An LSTM network is employed for classifying the extracted features. The reason for using this classifier is to take advantage of a dynamic classification algorithm, which uses the information in the extracted features as well as in their temporal structure. The inputs to the classifier are the sequence of vectorized graphs extracted from variable length segments. The LSTM network is comprised of three hidden layers where the first layer is a fully-connected layer consisting of 20 neurons, the second layer is an LSTM layer consisting of 20 neurons with a single-step delay feedback loop around the second hidden layer, and the third layer is a fully-connected layer consisting of 2 neurons. These layers are followed by softmax and classification layers. The classification accuracy is considered as the one obtained at the end of each trial.

III. RESULTS

In this study, 32 EEG channels covering the whole scalp were used. The extracted functional connectivity graphs were considered to be undirected. Accordingly, the graph matrices were symmetric and included no self-loops. As such, only the upper triangle from each graph matrix was used resulting in a feature vector of size 496 ($= \frac{32\times31}{2}$). To train and test the classifier for each motor imagery task, features extracted from both pain-free and under-pain conditions were divided into three randomized groups for training (70%), validation (15%), and testing (15%). Table. I summarizes the accuracy results for classifying pain-free versus under-pain conditions for each motor imagery task. An average classification accuracy (across subjects) of $79.43\%, 78.26\%, 80.04\%$, and 77.86% is achieved for the right hand, left hand, foot, and tongue motor imagery tasks, respectively.

The average classification accuracy results for each frequency band as well as for the un-decomposed EEG data are shown in Fig. 2. It can be seen that the highest average accuracy is achieved for the gamma band (84.16%), which is even higher than the case of using the un-decomposed EEG data (78.90%). This might be due to the presence of more non-discriminatory information from other bands when classification is performed using un-decomposed data as compared to data in the gamma band. The average accuracy from beta and alpha bands are 75.48% and 58.85%, respectively. In addition, for all motor imagery tasks, the average classification accuracy significantly decreases (approximately to the chance level) when graphs are extracted from the delta and theta bands. These results suggest that as compared to the gamma band, the functional connectivity graphs extracted from these lower bands, contribute less in discriminating between pain-free and under-pain motor imagery tasks. It should be noted that we cannot directly compare the results of this study with existing EEG pain studies, because they have mostly investigated pain-induced changes in resting state, whereas here, the brain is engaged in executing motor imagery tasks.

IV. DISCUSSIONS

In this study, we investigated whether motor imagery activities in pain-free and under-pain conditions can be distinguished in EEG data. We conducted motor imagery experiments to collect EEG recordings under both pain-free and pain conditions. Using our recently proposed method, we extracted functional connectivity graphs from quasi-stationary time intervals of EEG recordings. We used a LSTM artificial neural network to classify motor imagery

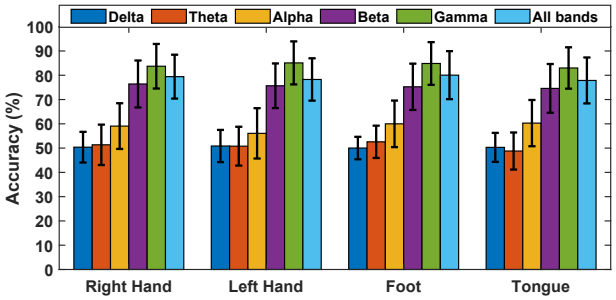

Fig. 2: Accuracy results for classifying different motor imagery tasks under pain-free versus pain conditions in different frequency bands.

classes corresponding to pain-free versus under-pain conditions. Our results indicated that the proposed method based on dynamic functional graphs can accurately differentiate various pain-free motor imagery tasks from their corresponding tasks with added pain. Therefore, this method can serve as reliable predictor to determine whether the motor imagery tasks are performed in pain-free or under-pain conditions. Moreover, our band-specific classification analysis showed that the highest accuracy was achieved from the gamma band, suggesting the relevance of gamma oscillations in the discrimination of motor imagery tasks associated with pain-free and pain conditions.

In the present study, we investigated classification of pain vs no-pain conditions in a task-based framework, for the first time. However, more tasks (e.g. cognitive tasks, etc.) should be studied to evaluate the generalizability of the proposed method in discriminating pain-free and under pain conditions. Alongside with these findings, the results of this study can be further extended to bring insights into the understanding of how the brain processes motor imagery tasks in the presence of the pain.

V. Conclusion and Future Work

In this paper, we used a functional connectivity-based method for discriminating motor imagery tasks under pain-free versus pain conditions. Results for classification accuracy demonstrated the effectiveness of the proposed method in differentiating motor imagery tasks performed with and without pain. Additionally, the classification results using different frequency bands revealed that the gamma band offers the highest average accuracy for this classification problem. Future work involves the development of motor imagery-based BCI algorithms which incorporate the pain detection capability and can adapt to the pain condition without affecting the classification performance.

Acknowledgment

The authors thank Jennifer Huang and Shiva Salsabilian for their help in the data collection process.

References

[1] U. Chaudhary *et al.*, "Brain–computer interface–based communication in the completely locked-in state," *PLoS Biology*, vol. 15, no. 1, p. e1002593, 2017.

[2] R. Abiri *et al.*, "A comprehensive review of EEG-based brain–computer interface paradigms," *Journal of Neural Engineering*, vol. 16, no. 1, p. 011001, 2019.

[3] A. Comaniciu *et al.*, "Enabling communication for locked-in syndrome patients using deep learning and an emoji-based brain computer interface," in *IEEE Biomedical Circuits and Systems Conference (BioCAS)*, 2018, pp. 1–4.

[4] G. R. Müller-Putz *et al.*, "Motor imagery-induced EEG patterns in individuals with spinal cord injury and their impact on brain–computer interface accuracy," *Journal of Neural Engineering*, vol. 11, no. 3, p. 035011, 2014.

[5] Y.-H. Liu *et al.*, "Motor imagery EEG classification for patients with amyotrophic lateral sclerosis using fractal dimension and fishers criterion-based channel selection," *Sensors*, vol. 17, no. 7, p. 1557, 2017.

[6] P. J. Siddall *et al.*, "A longitudinal study of the prevalence and characteristics of pain in the first 5 years following spinal cord injury," *Pain*, vol. 103, no. 3, pp. 249–257, 2003.

[7] R. Rupp, "Challenges in clinical applications of brain computer interfaces in individuals with spinal cord injury," *Frontiers in Neuroengineering*, vol. 7, p. 38, 2014.

[8] G. Misra *et al.*, "Automated classification of pain perception using high-density electroencephalography data," *Journal of Neurophysiology*, vol. 117, no. 2, pp. 786–795, 2017.

[9] C. Huishi Zhang *et al.*, "Spectral and spatial changes of brain rhythmic activity in response to the sustained thermal pain stimulation," *Human Brain Mapping*, vol. 37, no. 8, pp. 2976–2991, 2016.

[10] A. J. Furman *et al.*, "Cerebral peak alpha frequency predicts individual differences in pain sensitivity," *NeuroImage*, vol. 167, pp. 203–210, 2018.

[11] M. Vatankhah *et al.*, "Perceptual pain classification using ANFIS adapted RBF kernel support vector machine for therapeutic usage," *Applied Soft Computing*, vol. 13, no. 5, pp. 2537–2546, 2013.

[12] V. Vijayakumar *et al.*, "Quantifying and characterizing tonic thermal pain across subjects from EEG data using random forest models," *IEEE Transactions on Biomedical Engineering*, vol. 64, no. 12, pp. 2988–2996, 2017.

[13] A. Haddad *et al.*, "Early decoding of tongue-hand movement from EEG recordings using dynamic functional connectivity graphs," in *9th International IEEE/EMBS Conference on Neural Engineering (NER)*, March 2019, pp. 373–376.

[14] M. Ploner *et al.*, "Brain rhythms of pain," *Trends in Cognitive Sciences*, vol. 21, no. 2, pp. 100–110, 2017.

[15] https://sccn.ucsd.edu/eeglab/.

[16] E. L. Glassman, "A wavelet-like filter based on neuron action potentials for analysis of human scalp electroencephalographs," *IEEE Transactions on Biomedical Engineering*, vol. 52, no. 11, pp. 1851–1862, 2005.

[17] A. Haddad *et al.*, "Multi-scale analysis of the dynamics of brain functional connectivity using EEG," in *IEEE Biomedical Circuits and Systems Conference (BioCAS)*, 2016, pp. 240–243.

[18] A. E. Haddad *et al.*, "Global EEG segmentation using singular value decomposition," in *37th Annual International Conference of the IEEE Engineering in Medicine and Biology Society (EMBC)*, 2015, pp. 558–561.

[19] ——, "Source-informed segmentation: A data-driven approach for the temporal segmentation of EEG," *IEEE Transactions on Biomedical Engineering*, vol. 66, no. 5, pp. 1429–1446, 2019.

[20] W. R. Winter *et al.*, "Comparison of the effect of volume conduction on EEG coherence with the effect of field spread on MEG coherence," *Statistics in Medicine*, vol. 26, no. 21, pp. 3946–3957, 2007.

[21] C. Carvalhaes *et al.*, "The surface laplacian technique in EEG: Theory and methods," *International Journal of Psychophysiology*, vol. 97, no. 3, pp. 174–188, 2015.

[22] http://psychophysiology.cpmc.columbia.edu/Software/CSDtoolbox/.